Vol 15 No 4, April 2006
1009-1963/2006/15(04)/0859-07

Chinese Physics

© 2006 Chin. Phys. Soc.
and IOP Publishing Ltd

Microstructure and optical absorption of Au–MgF_2 nanoparticle cermet films*

Sun Zhao-Qi(孙兆奇)†, Cai Qi(蔡 琪), and Song Xue-Ping(宋学萍)

School of Physics and Material Science, Anhui University, Hefei 230039, China

(Received 19 December 2005; revised manuscript received 13 January 2006)

The microstructure and optical absorption of Au–MgF_2 nanoparticle cermet films with different Au contents are studied. The microstructural analysis shows that the films are mainly composed of the amorphous MgF_2 matrix with embedded fcc Au nanoparticles with a mean size of 9.8–21.4nm. Spectral analysis suggests that the surface plasma resonance (SPR) absorption peak of Au particles appears at λ=492–537nm. With increasing Au content, absorption peak intensity increases, profile narrows and location redshifts. Theoretical absorption spectra are calculated based on Maxwell-Garnett theory and compared with experimental spectra.

Keywords: nanoparticle cermet films, microstructure, optical absorption
PACC: 7865, 6860

1. Introduction

Cermet films that consist of metal nanoparticles embedded in ceramic matrix have been extensively studied because of their unique optical properties such as photoluminescence, third-order nonlinear optical and photocatalytic effect.[1−5] These novel properties caused by the quantum size effect show strong dependence on the size, shape and surface[6] of the particles, indicating that the volume fraction and microstructure of the embedded metal nanoparticles, together with the dielectric constant of the matrix, are the key factors that control the optical properties of the films.[7−10] Recently, a number of studies have been carried out: Chandonnet and Boivin[11] have studied the influence of the microstructure and composition on the optical constants of Cu–NaF_2, Ag–NaF_2, Cu–$PbCl_2$, and Ag–$PbCl_2$ cermet films; Evans[12] and Granqvist[13] have investigated the optical properties of Ag–SiO_x films and the effect of composition variation on Au–MgO as well as Au–Al_2O_3 films. Gajdardziska-Josifovaka *et al*[14] have measured the void fraction of Ag–MgF_2 films with different compositions by means of quartz crystal oscillation. Wang and Zhao[15] have studied the microstructure and optical properties of Cu–CaF_2 cermet film. Chen *et al*[16] have investigated the optical absorption and nonlinear response properties of Ag–SiO_2 cermet film. Shi *et al*[17] have studied microstructure and Raman spectra of Ag–MgF_2 cermet films. Wang *et al*[18] have investigated the morphology , element chemical state and absorption spectra of (Au, Fe)/$BaTiO_3$ nanocomposite thin films. Sun *et al*[19,20] have carried out a research on electrical properties of Cu–MgF_2 cermet films and optical constants of Ag–MgF_2 cermet films.

It is known that Au particles have a large third-order nonlinear susceptibility and pico-second near-resonance nonlinear response,[21] which implies their possible application in nonlinear optical devices.[22] The coarsening of Au particles increases the third-order optical susceptibility and absorption coefficient.[23] MgF_2, a typical material for optical coatings, with interesting physical and chemical properties such as high hardness, good stability in hostile environments, and a very low refractive index (n=1.38),[24] is widely used in various optical applications. So, cermet films composed of Au nanoparticles and MgF_2 matrix could be an attractive candidate for novel optical and optoelectronic devices. In addition, this kind of 'diffused' structure made up of metal nanoparticles diffused in the ceramic matrix is an ideal system to verify various effective medium the-

*Project supported by the National Natural Science Foundation of China (Grant No 59972001), the Natural Science Foundation of Anhui Province, China (Grant No 01044901), the Talent Foundation of Anhui Province, China (Grant No 2004Z029), and the Talent Development Foundation of Anhui University, Anhui Province, China.

†E-mail: szq@ahu.edu.cn

ories, which were established to interpret the optoelectronic behaviour of a metal nanoparticles/dielectric matrix system. Consequently, the investigation on the microstructure and optical properties of Au–MgF_2 cermet films can be of great significance for both theoretical and practical reasons. However, as we know, so far little work has been done on Au–MgF_2 cermet films.[25]

In this paper, Au–MgF_2 nanocrystalline cermet films are prepared by radio frequency (rf) magnetron co-sputtering, and the microstructure together with optical absorption over 200–800nm is analysed.

2. Experiments

Au–MgF_2 films were prepared by rf magnetron co-sputtering. The Au–MgF_2 target was made by sticking Au strips (99.99% purity) onto MgF_2 target (99.99% purity). Cermet films of about 70, 200 and 450nm in thickness were deposited onto formvar foil, Si(111) and quartz substrates, separately. After deposition, all the films were annealed in a high vacuum of 3×10^{-3}Pa for the purpose of crystallization. The Au volume fraction of the film can be calculated by the following formula:

$$q_M = xm_M\rho_D S_{MD}/(xm_M\rho_D S_{MD} + m_D\rho_M),$$
$$x = A_M/A_D, \qquad (1)$$

where q_M is Au volume fraction ; m_M and m_D are the mol masses of Au and MgF_2, respectively; ρ_M and ρ_D are the densities of Au and MgF_2, respectively; S_{MD} is the ratio of Au sputtering yield to that of MgF_2, and its experimental value is 9.7; x is the ratio of Au exposing area(denoted by A_M) to that of MgF_2 (denoted by A_D). Figure 1 shows the sectional diagram of Au–MgF_2 target, and detailed experimental deposition conditions are listed in Table 1.

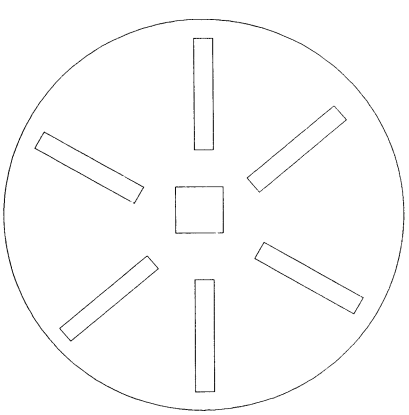


Fig.1. Schematic diagram of Au–MgF_2 target.

Table 1. Experimental deposition conditions.

Parameters	Values
Base vacuum /Pa	5.0×10^{-4}
Argon pressure /Pa	0.7
Sputtering power /W	60
Self-biased voltage /V	≈ -580
Film depositing rate /(nm/min)	≈ 8
Substrate temperature /K	≈ 293
Target-to-substrate distance /mm	60.0
Au volume fraction /vol.%	6, 15, 25, 40, 50, 60
Annealing vacuum /Pa	5.0×10^{-3}
Annealing temperature /°C	350
Annealing time /min	40

A MAC M18XHF-type x-ray diffractometer, a JEM-100SX transmission electron microscope, and a VG ESCALAB MK-II x-ray photoelectron spectroscope were employed to examine the microstructure and composition of Au–MgF_2 cermet films. A Shimadzu UV-240 ultraviolet-visible spectrophotometer was used to analyse the optical absorption of the films over 200–800nm.

3. Results and discussions

3.1. Composition analysis

To determine the composition of the prepared Au–MgF_2 films, the x-ray photoelectron spectroscopy (XPS) was adopted. An XPS survey spectrum of the nominal 60vol.% Au–MgF_2 film on Si substrate is presented in Fig.2. Calibrating by C1s (binding energy 284.40eV), the binding energies together with atomic percentages of O1s, Au4f, F1s, and Mg2p photoelectrons are 531.15eV (12.17at.%), 83.95eV (40.63at.%), 686.40eV (26.17at.%) and 50.75eV (12.61at.%), respectively. From the above data, a volume fraction of 62.6% for Au content in the film can be calculated, which approximates to the designed volume ratio.

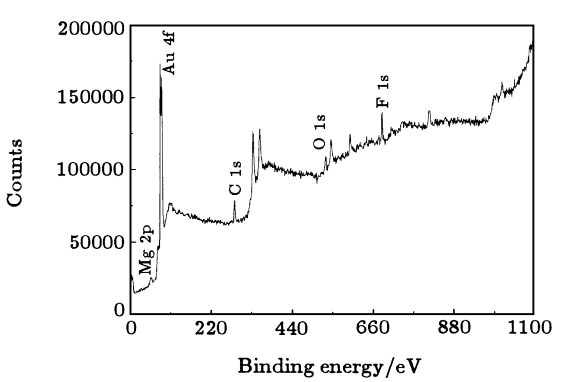


Fig.2. XPS of the nominal 60vol.% Au–MgF_2 cermet film.

3.2. Microstructure analysis

The XRD patterns of 6, 15, 25, 40, 50 and 60vol.% Au–MgF_2 cermet films on Si substrates are shown in Fig.3. The existence of both Au and MgF_2 diffraction peaks indicates that Au and MgF_2 contents in the prepared films keep their crystal structures (fcc and tetragonal).

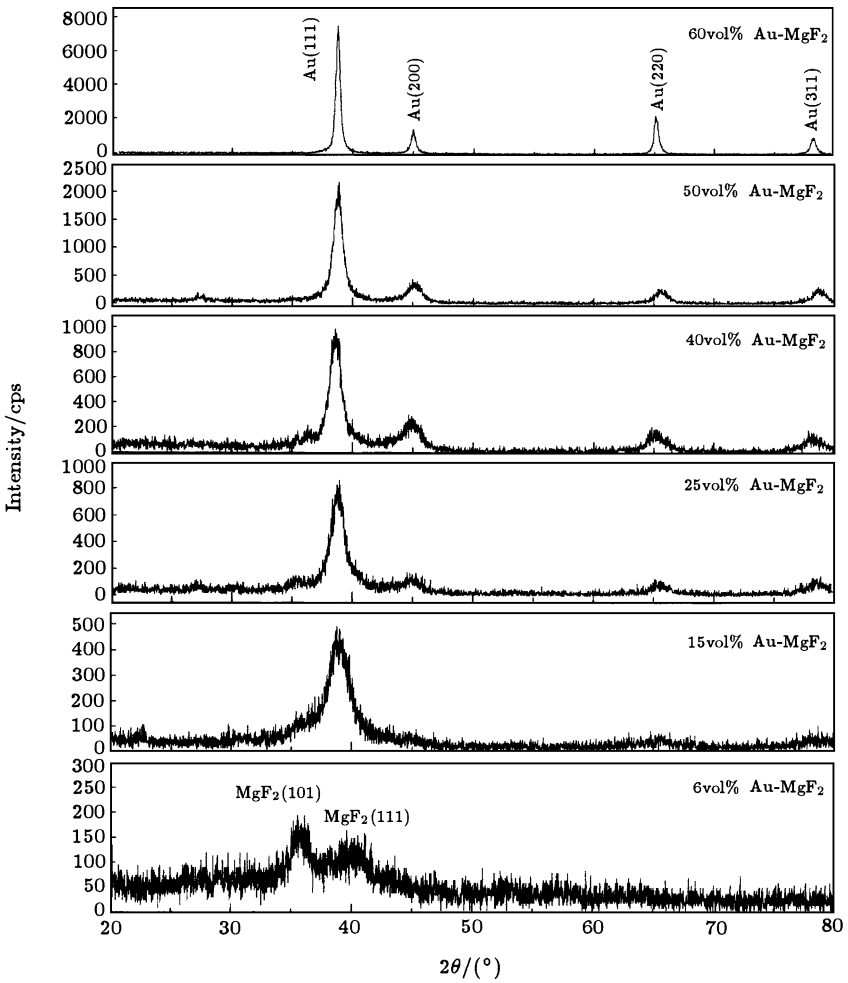


Fig.3. XRD patterns of Au–MgF_2 films with different compositions.

With increasing Au content, the peak intensity of MgF_2 decreases, while that of Au increases. However, only two weak diffraction peaks of MgF_2 can be observed, suggesting that the MgF_2 content in the films deposited on Si(111) at room temperature is mainly amorphous.

From Scherrer's formula

$$D = K\lambda/\beta\cos\theta, \tag{2}$$

where K is 0.9, λ is 1.54056Å, β is full width at half maximum (FWHM) of diffraction peak and θ is diffraction angle, the value of Au average grain size can be calculated from Fig.3.

From the Bragg function

$$2d\sin\theta = \lambda, \tag{3}$$

$$d = a/\sqrt{h^2+k^2+l^2}, \tag{4}$$

the value of the lattice constant of Au can be calculated, and the results are listed in Table 2.

Table 2. Microstructural parameters of Au particles in Au–MgF_2 cermet films.

Samples	Lattice constant/Å	Average grain size/nm
6vol.%Au–MgF_2	—	—
15vol.%Au–MgF_2	3.998	5.1
25vol.%Au–MgF_2	4.008	6.5
40vol.%Au–MgF_2	4.024	7.6
50vol.%Au–MgF_2	4.061	10.2
60vol.%Au–MgF_2	4.074	21.2

When Au volume fraction increases from 15% to 60%, the average grain size of Au particles increases from 5.1 to 21.2nm, while the Au lattice constant increases gradually from 3.998 to 4.074Å. Compared with the standard value (4.079Å) of bulk Au, the lattice constant of Au content in the film is smaller, which could be caused by the small size, large specific surface area and high surface energy of Au particles in the Au–MgF_2 cermet films.

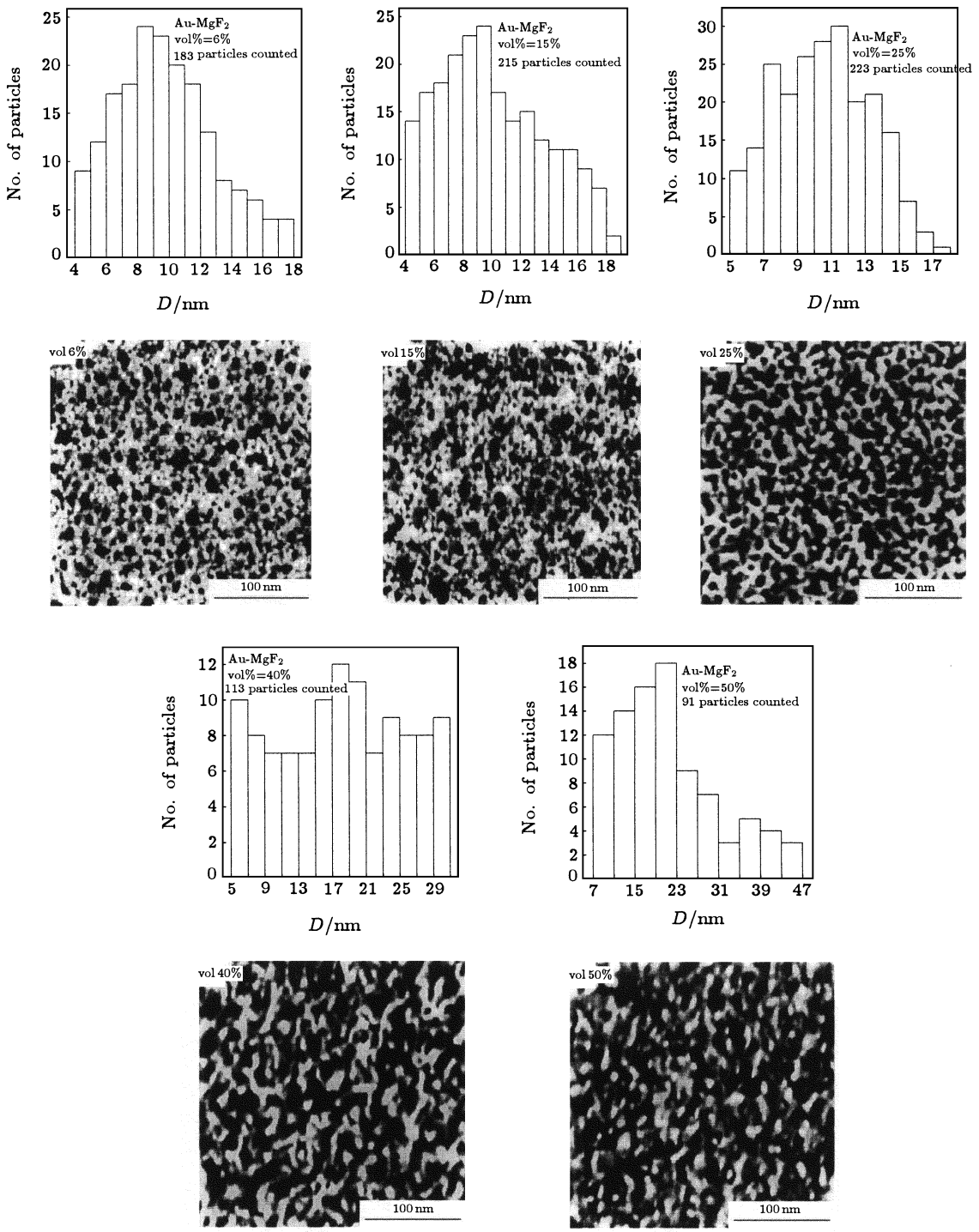


Fig.4. TEM micrographs and histograms of particle size distribution of Au–MgF_2 films.

Figure 4 presents the transmission electron microscopy (TEM) bright-field micrographs and the particle size distribution histograms of 6, 15, 25, 40 and 50vol.% Au–MgF_2 films on formvar foils. As shown in the TEM micrographs, dark-coloured Au particles are roughly spherical in shape and embedded in the MgF_2 matrix. With increasing Au content, the particle distribution density increases and the films transit gradually from the discrete state to the network one. Particle size distribution analysis suggests that the mean size of Au particles increases from 9.8 to 21.4nm with Au volume fraction increasing from 6% to 50%, and the details are listed in Table 3.

Table 3. Mean size of Au particles in Au–MgF_2 films.

Samples	Mean particle size/nm
6vol.%Au–MgF_2	9.8
15vol.%Au–MgF_2	10.2
25vol.%Au–MgF_2	10.5
40vol.%Au–MgF_2	18.1
50vol.%Au–MgF_2	21.4

3.3. Optical absorption properties

The optical absorption spectra over 200–800nm of 6vol.%–50vol.% Au–MgF_2 cermet films on quartz substrates are shown in Fig.5. Owing to 5d to 6sp interband transition by absorbing photons of energy higher than 2.76eV,[26] the films exhibit an increasing absorption in short wavelength region (<450nm). The SPR absorption peaks of Au particles for 15, 25, 40 and 50vol.% Au–MgF_2 cermet films occur at 492, 510, 522 and 537nm, respectively. Moreover, with increasing Au content, the SPR peak intensity increases, profile narrows and location redshifts.

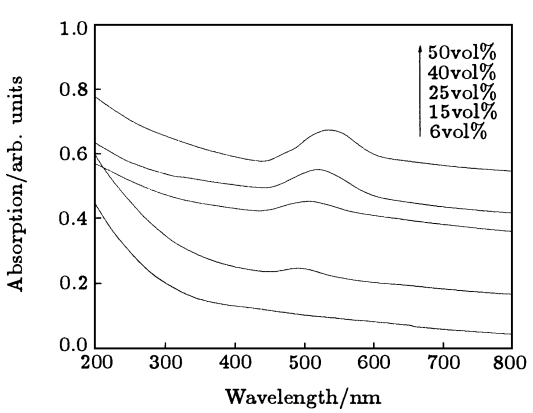


Fig.5. Experimental optical absorption spectra of Au–MgF_2 cermet films.

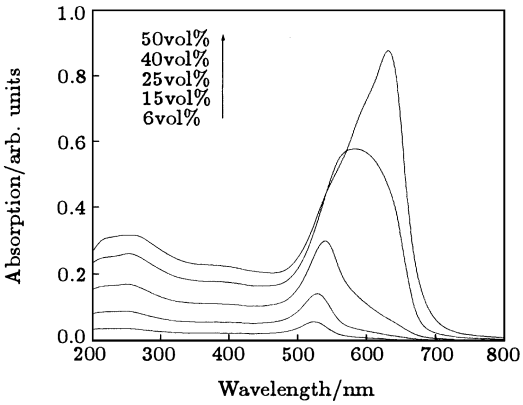


Fig.6. Theoretical optical absorption spectra of Au–MgF_2 cermet films.

The SPR absorption caused by an induced charge density oscillation exists in a dispersed system composed of metal particles embedded uniformly in a dielectric matrix. For such a dispersed system, assuming: 1) the interaction of particles can be neglected; 2) particles are spherical shaped; and 3) particles have the same size and space distribution, we can obtain the effective dielectric constant ε_{eff} by using Maxwell-Garnett formula[27]

$$\varepsilon_{\text{eff}} = (\varepsilon_{\text{m}}(1+2q) + 2\varepsilon_{\text{d}}(1-q)) \cdot \varepsilon_{\text{d}}/(\varepsilon_{\text{m}}(1-q) + \varepsilon_{\text{d}}(2+q)) = \varepsilon'_{\text{eff}} + \text{i}\varepsilon''_{\text{eff}}, \quad (5)$$

where ε_{m} is the complex dielectric constant of metal particles, ε_{d} is the dielectric constant of matrix, and q is the volume fraction of metal particles. Within the optical range, the relationship between the effective dielectric constant ε_{eff} and the complex optical refractive index N is

$$N = n + ik = \sqrt{\varepsilon_{\text{eff}}}, \quad (6)$$

where n represents the refractive index which stands for the dispersion of the system, and k represents the extinction coefficient which characterizes the absorption of the system. Using Eqs.(5)–(6), we can obtain

$$k = \sqrt{(|\varepsilon_{\text{eff}}| - \varepsilon'_{\text{eff}})/2}, \quad (7)$$

The absorption coefficient α of the system then can be obtained from the following formula

$$\alpha = 4\pi k/\lambda, \quad (8)$$

where λ is the wavelength of the incident light.

By combining Eqs.(5)–(8), the absorption coefficients of 6, 15, 25, 40 and 50vol.% Au–MgF_2 cermet films over 200–800nm can be calculated and are plotted in Fig.6. Compared the theoretical (Fig.6) and

the experimental spectra (Fig.5), the following points can be obtained:

1) In the theoretical spectra, for 6, 15, 25, 40 and 50vol.% Au–MgF_2 cermet films, the SPR absorption peaks of Au nanoparticles appear at 524, 528, 540, 580 and 630nm, respectively, while in the experimental spectra, the peaks appear at 492 (for 15vol.%), 510 (for 25vol.%), 522 (for 40vol.%) and 537 (for 50vol.%). A red shift of the peak location exists both experimentally and theoretically, which is attributed to an increase in the Au particle size with increasing Au content. The experimental peak location together with its red-shift amount, however, is different from the theoretical one, which could result from the small size effect on dielectric constants of Au nanoparticles in the films.

2) Obviously, in the experimental spectra, the SPR peak intensity is weaker and its profile is wider than in the theoretical spectra, especially for 6vol.% cermet film, the broadening of the experimental peak is large enough to make the SPR peak absent. In fact, Maxwell-Garnett theory[27] assumes all the metal particles have the same size; however, a size variation of the Au nanoparticles in the prepared films does exist (according to the particle size distribution histograms), which can lead to the broadening of SPR absorption peak, for different-sized particles have different SPR frequencies.

3) The theoretical calculation assumes that all particles in the film are spherical shaped, but not all Au particles in the prepared films are spherical (according to the TEM micrographs), so the shape and space variation of Au particles exists, which has an important influence on the location, intensity and width of the SPR peak of a cermet film.[28] Moreover, the existence of voids in Au–MgF_2 cermet films, which will influence the dielectric properties of the system, actually makes the film a three-phase system, but the Maxwell-Garnett theory can only be valid for a two-phase system. So, further detailed work is necessary, for a more accurate interpretation on the unique photoelectronic behaviour of a cermet film.

4. Conclusions

1. The 6vol.%–60vol.% Au–MgF_2 nanoparticle cermet films were successfully prepared by rf magnetron co-sputtering. Microstructure analysis shows that the cermet films are mainly composed of the amorphous MgF_2 matrix with embedded fcc Au nanoparticles with average sizes of 9.8–21.4nm. XPS analysis of nominal 60vol.% Au–MgF_2 cermet film suggests that Au volume fraction is 62.6%, which approximates to the designed volume ratio.

2. The experimental optical absorption spectra of the films over 200–800nm show that the SPR absorption peaks of Au nanoparticles for 15, 25, 40 and 50vol.% Au–MgF_2 cermet films appear at 492, 510, 522 and 537nm, respectively. The interband transition absorption of Au begins when the wavelength is shorter than 450nm. With increasing Au content, the SPR peak intensity increases, profile narrows and location redshifts.

3. The theoretical optical absorption spectra have been calculated based on Maxwell-Garnett theory. The theoretical results are quantitatively consistent with the experimental ones, and the discrepancy between them is attributed to the existence of particle size distribution, particle shape and space distribution, as well as voids in the prepared Au–MgF_2 cermet films.

References

[1] Joudrier V, Bourdon P, Hache F and Flytzanis C 1998 *Appl. Phys.* B **67** 627

[2] Hayashi S, Kataoka M and Yamamoto K 1993 *Jpn. J. Appl. Phys.* **32** L274

[3] Beydoun D, Amal R, Low G and McEvoy S 1999 *J. Nanopart. Res.* **1** 439

[4] Wang W T, Yang G, Chen Z H, Zhou Y L, Lü h B and Yang G Z 2002 *Chin. Phys.* **11** 1324

[5] Shen H, Cheng B L, Lü G W, Wang W T, Guan D Y, Chen Z H and Yang G Z 2005 *Chin. Phys.* **14** 1915

[6] Wang Y and Herron N 1991 *J. Phys. Chem.* **95** 525

[7] Dalacu D and Martinu L 1999 *J. Vac. Sci. Technol.* A **17** 877

[8] Magruder R H III, Wittig J E and Zuhr R A 1993 *J. Non-Cryst. Solids* **163** 162

[9] White C W, Zhou D S, Budai J D, Zuhr R A, Magruder R H and Osborne D H 1994 *Mat. Res. Soc. Symp. Proc.* **316** 499

[10] Magruder R H III, Yang L, Haglund R F, White C W, Dorsinville R and Alfano R R 1993 *Appl. Phys. Lett.* **62** 1730

[11] Chandonnet A and Boivin G 1989 *Appl. Opt.* **28** 717

[12] Evans D 1985 *Phys. Rev.* B **32** 4169

[13] Granqvist C G 1979 *J. Appl. Phys.* **50** 2916

[14] Gajdardziska-Josifovaka M, McPhedran R C, Cockayne P J H, McKenzie D R and Collins R E 1989 *Appl. Opt.* **28** 2736

[15] Wang H and Zhao Z Q 1998 *J. Vac. Sci. Technol.* **18** 142 (in Chinese)

[16] Chen Z H, Xing G G and Chi G M 1999 *J. Wuhan Univ.* **45** 81 (in Chinese)

[17] Shi S H, Cao Z L and Sun Z Q 2003 *Chin. Opt. Lett.* **1** 305

[18] Wang W T, Yang G, Guan D Y, Wu W D and Chen Z H 2004 *Acta Phys. Sin.* **53** 932 (in Chinese)

[19] Sun Z Q, He Y P, Song X P and Sun D M 2003 *Acta Phys. Sin.* **52** 1455 (in Chinese)

[20] Sun Z Q and Sun D M 2004 *Chin. Opt. Lett.* **2** 243

[21] Fukumi K, Chayahara A, Kadono K, Sakaguchi T, Horino Y, Miya M, Hayakawa J and Satou M 1991 *Jpn. J. Appl. Phys.* **30** L742

[22] Fukumi K, Chayahara A, Kadono K, Sakaguchi T, Horino Y, Miya M, Fuji K, Hayakawa J and Satou M 1994 *J. Appl. Phys.* **75** 3075

[23] Ricard D, Roussignol P and Flytzanis C 1985 *Opt. Lett.* **10** 511

[24] Palik E D 1985 *Handbook of Optical Constants of Solid* (Orlando: Harcount) p913

[25] Lissberger P H and Nelson R G 1974 *Thin Solid Films* **21** 159

[26] Vazquez-Cuchillo O, Pal U and Vazquez-Lopez C 2001 *Sol. Energy Mater. Sol. Cells* **70** 369

[27] Maxwell-Garnett J C 1904 *Phil. Trans. R. Soc.* A **203** 385

[28] Cohen R W, Cody G D and Coutts M D 1973 *Phys. Rev. Lett.* **8** 3689